Article

Comparative Genomics Analysis of *Ganoderma* Orthologs Involved in Plant-Pathogenesis

Chai-Ling Ho

Faculty of Biotechnology and Biomolecular Sciences, Universiti Putra Malaysia (UPM),
Serdang 43400, Selangor, Malaysia; clho@upm.edu.my

Abstract: *Ganoderma* species are producers of bioactive secondary metabolites and lignin degraders. A few *Ganoderma* species are known to be plant pathogens that attack economically important trees. In this study, comparative genomics analysis was conducted on the proteome of ten *Ganoderma* species/strains, focusing on the proteins that have been reported to be involved in plant-pathogenesis in other fungi. Fungal trophic lifestyle prediction of these *Ganoderma* species/strains supported that *G. boninense* (a potent pathogen to oil palm) is a hemibiotrophic fungus while the other *Ganoderma* species/strains analyzed were predicted to be saprophytes or a symbiont based on their Carbohydrate-Active Enzyme (CAZyme) contents. Although these *Ganoderma* species/strains were demonstrated to share many CAZymes and secondary metabolite core gene clusters, individual species may produce unique CAZymes and secondary metabolite core genes that determine their lifestyles, host-specificity, and potential as a producer of bioactive secondary metabolites. Ortholog groups that are related to fungal virulence from seven *Ganoderma* species/strains including those involved in lignin degradation, mycotoxin, siderophore and ergosterol biosynthesis, and virulence were summarized. Potential effectors were predicted from the proteome of these *Ganoderma* species/strains, and putative effectors that were being expressed in *G. boninense* in oil palm roots but not found in other species were identified. The findings provide a useful resource to further analyze plant-pathogenesis and wood degradation activities of these *Ganoderma* species.

Keywords: effector prediction; *Ganoderma*; orthologs; plant-pathogenesis

1. Introduction

The genus *Ganoderma* (Ganodermataceae; Polyporales) consists of more than 300 species of widely distributed wood-decaying fungi [1]. While some are saprophytes that feed on dead wood, others are hemibiotrophic pathogens that decompose living hardwood trees, such as conifers, rubber trees, oil palms, and coconut palms [2–4] by producing lignin- and cellulose-degrading enzymes. *Ganoderma* species are also featured as producers of secondary metabolites (mainly triterpenes such as ganoderic acids), oligosaccharides, polysaccharides, polysaccharide–peptide complex, phenols, and steroids that have potential bioactivities [1,5–8]. A few *Ganoderma* species, such as *G. lucidum* and *G. sinense*, have been used in traditional medicine [9,10]. The transcript sequences for enzymes related to the biosynthesis of terpenes [11–13] and ganoderic acids [14] have been identified. The expression of genes in the mevalonate pathway has also been profiled [15–17]. The wood-decaying capacity and pathogenicity of *Ganoderma* species is associated with the ability of these fungi to produce plant-cell-wall degrading enzymes. The gene sequences encoding carbohydrate-active enzymes (CAZymes) were identified from the genome assembly of *G. boninense* strain NJ3, *G. boninense* strain G3, *G. australe*, *G. leucocontextum*, *G. lingzhi*, *G. sinense*, and *G. tsugae* [11,13,18]. The transcript sequence and abundance of a few manganese peroxidases and laccases from *G. boninense* PER71 have also been reported [19], following the identification of these transcripts in the transcriptome of infected oil palm [20]. In addition, the purification and characterization of laccases from different

Ganoderma strains [21–25], recombinant manganese peroxidases [26], and laccases from *G. lucidum* and *G. australe* [27–29] were reported. Other transcripts related to pathogenesis that have been characterized include the necrosis and ethylene inducing protein (NEP)-like protein and cyclophilin from *G. boninense* [30,31], while the sequences of hydrophobins from different *Ganoderma* species were reported by Sulaiman et al. [32].

As of March 2023, 17 genome resources from eight *Ganoderma* species were available in the National Center for Biotechnology Information (NCBI) database compared to 12 genome assemblies from six *Ganoderma* species in March 2022. However, only the full suite of annotated proteins from *G. sinense* [33] and *G. leucocontextum* Dai12418 [34] were available in NCBI, while the predicted proteins from the nuclear genomes of other *Ganoderma* species remained unpublished, unknown, or no longer accessible from the portals mentioned in publications [14,17,32]. In addition, a total of 5957 predicted protein sequences from *G. boninense* strain NJ3 were deposited by Ramzi et al. [18] in NCBI. Kües et al. [14] compared the genome sequence data of three *Ganoderma* species, i.e., *Ganoderma* sp. 10,597 [35], *G. lucidum* strain Xiangnong No. 1 [36], and *G. lucidum* strain G260125-1 [15], focusing on the sequence analysis of proteins belonging to the CYP450 family and in the mating loci *matA* and *matB* from these *Ganoderma* species/strains. Recently, the phylogenomic and comparative genomics of a few *Ganoderma* species focusing on genes involved in terpene metabolism and gene encoding secreted proteins were also reported [12,13,18]. In another recent paper, Khairi et al. [37] reported the predicted effector proteins from three *G. boninense* strains. Nevertheless, comparative genomics analyses of *Ganoderma* species, especially on proteins involved in plant-pathogenesis, are still limited.

Hence, the current study focused on the comparative genomics of putative orthologs that participate in plant-pathogenesis and wood degradation from ten *Ganoderma* species/ strains. Orthologs that could potentially contribute to fungal virulence and pathogenesis of seven *Ganoderma* strains in five different species were also identified and analyzed. The findings could serve as an impetus for future molecular cloning and characterization of genes from these *Ganoderma* species.

2. Materials and Methods

2.1. Retrieval of Genome Assemblies and Protein Sequences

The genome assemblies of *Ganoderma* species (*G. boninense* strain G3 GCA_002900995.2; *G. boninense* strain NJ3 GCA_001855635.1; *G. lucidum* strain BCRC36111 GCA_012655175.1; *G. lucidum* strain BCRC37177 GCA_000338035.1; *G. lucidum* strain G260125-1 GCA_000262775.1; *G. lucidum* strain Xiangnong No.1 GCA_000271565.1; *G. multipileum* GCA_000338015.1; *G. sinense* ZZ0214-1 GCA_002760635.1; *G. tsugae* GCA_003057275.1; and *Ganoderma* sp. BRIUMSc GCA_008694245.1) and the annotated protein sequences of *G. sinense* ZZ0214-1 were retrieved from GenBank in December 2020. Table S1 shows the summary of the *Ganoderma* species, strains, hosts, and other information.

2.2. Gene Prediction from Ganoderma Species

The genome assembly and reference protein sequences of *G. sinense* ZZ0214-1 were submitted to WebAUGUSTUS Service (http://bioinf.uni-greifswald.de/webaugustus/ index.gsp; accessed on 9 December 2020) as a training gene set to generate training species-specific parameters. Gene prediction from the other *Ganoderma* species was conducted in WebAUGUSTUS by using the training species-specific parameters obtained for *G. sinense* ZZ0214-1. The completeness of predicted proteome was evaluated by the Benchmarking Universal Single-Copy Orthologs (BUSCO) tool [38] with the polyporales_odb10 database.

2.3. Functional Annotation

BLAST2GO was used for the functional annotation of predicted proteins from *Ganoderma* species by assigning Gene Ontology identifier (GO ID), EC number, and pfam to the query sequences. Blast2GO [39] was conducted with a minimum cut-off of 10^{-5} for BlastP against the SwissProt database and default parameters set by OmicsBox (www.biobam.com

accessed on 27 March 2021), i.e., annotation cut-off (55), GO-weight (5), HSP-hit coverage cut-off (0), and apply no filter GO by taxonomy. GO enrichment using Fisher's exact test ($p < 0.01$, FDR <0.05) was performed in OmicsBox. A KEGG Orthology (KO) identifier (K number) was assigned to the sequence by GHOSTX searches in GhostKOALA (www.kegg.jp/ghostkoala/; accessed on 27 March 2021; [40]), respectively, against the "genus_prokaryotes+family_eukaryotes" database in Kyoto Encyclopedia of Genes and Genomes (KEGG).

2.4. Identification of Secondary Metabolite Gene Clusters, CAZyme and Classification of Fungal Lifestyles

The secondary metabolite gene clusters were identified by antiSMASH fungal version v6.0 [41] from each *Ganoderma* species/strain using the standard (recommended) parameters at the antiSMASH webserver (https://fungismash.secondarymetabolites.org/; accessed on 2 August 2022). CAZymes were identified using hmmscan in HMMER 3.0 [42] with the "-domtblout" parameter, followed by the shell/perl script "hmmscan-parser.sh" in dbCAN ver. 6 [43] with a minimum alignment length of 80 amino acids, E-value < 10^{-5}, and >30% coverage of HMM and included in a prediction tool known as CAZyme-Assisted Training And Sorting of trophy (CATAStrophy) [44]. The trophic lifestyles of *Ganoderma* species/strains were inferred according to CAZyme content by CATAStrophy. Principal component analysis (PCA) of CAZyme contents in CATAStrophy allowed the separation of most of the species/strains with the first two principal components (PCs). Hence, PC1 and PC2, which separated most of the species according to lifestyles (biotrophs, hemibiotrophs, necrotrophs, saprotrophs, and symbionts), were plotted in Excel for visualization.

2.5. Ortholog Analysis

Orthologs were identified by OrthoMCL (https://orthomcl.org/; [45] in OrthoVenn (https://orthovenn2.bioinfotoolkits.net/home; accessed on 14 February 2021; [46]) at an E-value of 10^{-5}. Ortholog clusters related to virulence and pathogenesis were identified by keyword search or GO IDs. The Venn diagrams were drawn with InteractiVenn (http://www.interactivenn.net/index.html; accessed on 18 February 2021; [47]).

2.6. Prediction of Effector Sequences

Phobius (http://phobius.sbc.su.se/instructions.html; accessed on 13 March 2021; [48]) was used to predict fungal proteins with trans-membrane topology and signal peptide. EffectorP ver 2.0 (http://effectorp.csiro.au/; accessed on 17 March 2021; [49]) was used for the prediction of putative effector sequences from the putative protein sequences of *Ganoderma* species with transmembrane topology and signal peptide. Protein sequences that have BlastP matches against the SwissProt database with an E-value of 10^{-5} or less were considered to be significant. Fisher's exact test ($p < 0.01$, FDR < 0.05) was conducted to identify the GO terms that were enriched among the predicted effectors in each *Ganoderma* species.

Identification of putative effectors that were present in oil palm infected by *G. boninense* (G) and *Trichoderma* (T) was performed by mapping the RNAseq data (European Nucleotide Archive (ENA) accession number: PRJEB7252) of a previous transcriptome study [20] to the genes of *G. boninense* strain G3 in OmicsBox (www.biobam.com; accessed on 4 April 2021).

3. Results

3.1. Prediction of Proteins of Ganoderma Species/Strains

Since *G. sinense* is the only *Ganoderma* species with annotated proteins among the *Ganoderma* genomes retrieved from NCBI when this study was conducted, the proteins from other *Ganoderma* genome assemblies were predicted with the protein sequences of *G. sinense* as a training set. The number of predicted proteins ranged from 11,040 in *G. lucidum* G260125-1 to 21,487 from *G. boninense* strain NJ3. The numbers of predicted proteins from the two *G. boninense* genome assemblies, i.e., *G. boninense* strain G3 and *G. boninense* strain NJ3, were comparable to those reported by an independent group [37]

on the same strains. Based on BUSCO analysis, the completeness of the predicted proteomes of *G. lucidum* strain BCRC37177, *G. multipileum,* and *G. sinense* ZZ0214-1 was more than 90% while the completeness of the predicted proteomes of *G. boninense* strain NJ3 and *Ganoderma* sp. BRIUMSc was only 66%–69% (Table 1), mainly due to the presence of a high number of fragmented and missing proteins (Table 1).

Table 1. The number of predicted proteins, completeness of the predicted proteome, and percentage of genes with BlastP matches to SwissProt database ($\leq 10^{-5}$), GO, and KO annotations.

Species	Number of Predicted Proteins in the Genome	Completeness of Proteome Predicted by BUSCO					Functional Annotations		
		% Complete BUSCOs (C)	% Complete and Single-Copy BUSCOs (S)	% Complete and Duplicated BUSCOs (D)	% Fragmented BUSCOs (F)	% Missing BUSCOs (M)	% Genes with BlastP Matches	% Genes with BlastP Matches That are Mapped to GO	% Genes with KO Annotation
G. boninense G3	20,564	82.6	66.7	15.9	5.3	12.1	47.95	47.93	28.08
G. boninense NJ3	21,487	66.7	63.6	3.1	10.9	22.4	39.47	39.47	24.46
G. lucidum G260125-1	11,040	87.7	86.9	0.8	3.6	8.7	57.48	57.45	34.02
G. lucidum Xiangnong	12,342	89.4	88.6	0.8	1.9	8.7	53.82	53.80	30.46
G. lucidum BCRC36111	12,843	75	71.1	3.9	7.8	17.2	52.93	52.90	32.04
G. lucidum BCRC37177	12,533	90.5	89.8	0.7	2.9	6.6	54.62	54.61	31.86
G. multipileum	13,358	90.6	89.8	0.8	2.9	6.5	53.18	53.17	30.87
G. sinense ZZ0214-1	15,478	90.1	89.0	1.1	5.0	4.9	47.83	47.70	27.08
G. tsugae	15,426	83.5	79.9	3.7	5.6	10.9	48.17	48.15	28.90
Ganoderma sp. *BRIUMSc*	18,612	68.8	64.3	4.5	12.7	18.5	47.67	47.65	29.76

Table 1 also shows the number of proteins with significant matches to SwissProt database ($\leq 10^{-5}$), GO, and KO annotations from each *Ganoderma* species or strain. The number of proteins with BlastP matches from each species/strain ranges from 39%–57%. Almost all the proteins with BlastP matches were assigned with at least one GO ID. The number of genes with KO from each species/strain ranges from 24%–32%. The four *G. lucidum* strains and *G. multipileum* were found to have a higher number of annotated proteins compared to other species/strains. *G. boninense* strain NJ3 has the lowest number of annotated proteins, possibly due to fragmented genes or incomplete genome sequencing data (Table 1).

3.2. CAZymes and Classification of Prediction of Fungal Lifestyles

Figure 1 shows the CAZyme content in *Ganoderma* species/strains. The *G. boninense* strain G3 was found to have the highest number of CAZymes (Figure 1A), especially those in the glycosyl hydrolase (GH) family and glycosyl transferase (GT) family. The CAZymes in the GH family dominated the predicted CAZymes from all *Ganoderma* species/strains, followed by CAZymes with auxiliary activities (AA) and GT activities (Figure 1B). The three most prominent GH families among all *Ganoderma* species/strains were GH18 (including chitinases Classes III and V and xylanase inhibitor), GH16_1 (including xyloglucan:xyloglucosyltransferase), and GH3 (including β-glucosidase). A few enzymes seemed to be unique to one or a few *Ganoderma* species/strains, including GH13 enzyme (possibly with α-amylase or sucrose phosphorylase activity), which was only found in *G. boninense* strain G3, and GH5 (endo-β-1,4-glucanase/cellulase), which was only found in *G. lucidum* strain BCRC37177 and *G. multipileum*. A few CAZymes were found to be missing from *G. boninense* strains, including GH43-33 (α-L-arabinofuranosidase), GH45 (xyloglucan-specific endo-β-1,4-glucanase or endo-β-1,4-mannanase), and GH99 (mannan endo-1,2-α-mannanase).
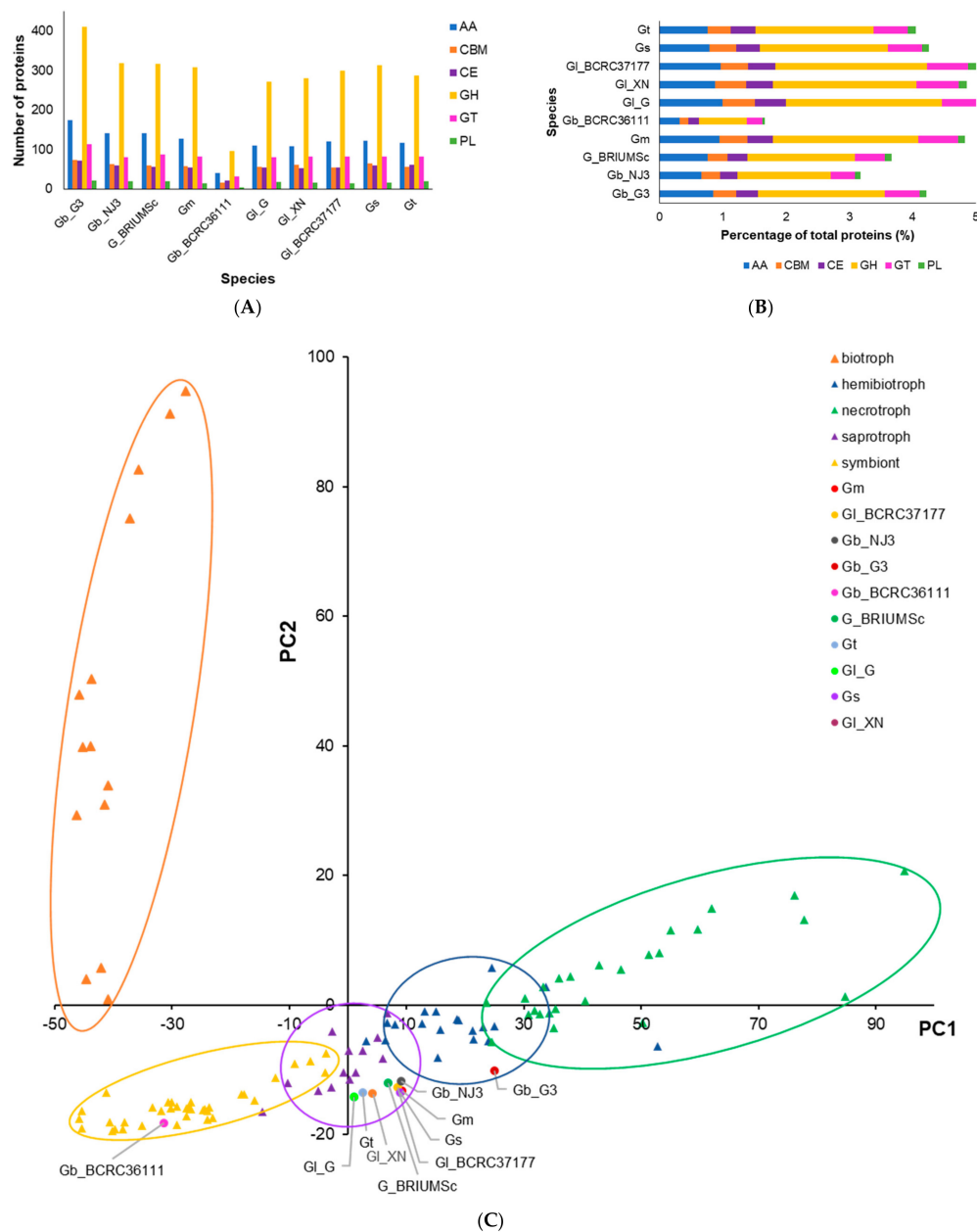
Figure 1. Carbohydrate-active enzyme (CAZyme) content among *Ganoderma* species/strains. (**A**), Number of CAZymes of each species/strain according to CAZyme superfamily: glycoside hydrolase (GH), glycosyl transferase (GT), auxiliary activity (AA), carbohydrate esterase (CE), polysaccharide lyase activity (PL), and carbohydrate-binding modules (CBM); (**B**), Percentage of CAZymes of each species/strain according to CAZyme superfamily; (**C**), Principal-component analysis (PCA) plot of fungal lifestyle predictions as inferred by CATAStrophy. PC1, principal component 1, and PC2, principal component 2. The plot shows the CAZyme-inferred phenotypic trophisms of 85 reference species of fungi with different lifestyles (i.e., 14 biotrophs, 20 hemibiotrophs, 25 nectrotrophs, 13 saprotrophs, and 36 symbionts in a training set used by CATAStrophy) and *Ganoderma* species/strains. Gb_G3, *G. boninense* strain G3; Gb_NJ3, *G. boninense* strain NJ3; Gm, *G. multipileum*; Gl_G, *G. lucidum* strain G260125-1; Gl_ BCRC36111, *G. lucidum* strain BCRC36111; Gl_ BCRC37177, *G. lucidum* strain BCRC37177; Gl_XN, *G. lucidum* strain Xiangnong; Gs, *G. sinense*; Gt, *G. tsugae*; G_BRIUMSc, *Ganoderma* sp. BRIUMSc. The groupings of biotrophs, hemibiotrophs, nectrotrophs, saprotrophs, and symbionts are shown by orange, blue, green, purple, and yellow circles, respectively.

The AA class CAZymes were dominated by a few subclasses, such as the AA3_2 (including both aryl alcohol oxidase and glucose 1-oxidase in the glucose-methanol-choline oxidoreductases family with flavin-adenine dinucleotide (FAD)-binding domain), AA9 (copper-dependent lytic polysaccharide monooxygenases), AA1_1 (laccases), AA2 (class II lignin-modifying peroxidases), and AA7 (gluco- or chito- oligosaccharide oxidase, cellooligosaccharide dehydrogenase), while the GT class CAZymes have many enzymes belonging to subclasses GT2 (especially GT2_ Chitin_synth_2), GT1, and GT8. All *Ganoderma* species/strains were classified as saprotrophs by CATAStrophy according to their CAZyme contents (Figure 1C), except *G. boninense* strain G3, which was identified as a hemibiotroph and *G. lucidum* strain BCRC36111, which was predicted to be a symbiont. However, the PCA plot of PC1 and PC2 which separated most of the species according to lifestyles shows some overlap between the neighboring clusters, except for the biotroph cluster (Figure 1C).

3.3. Secondary Metabolite Production Potential of Ganoderma Species

The secondary metabolite production potential of the *Ganoderma* species/strains was inferred from the putative biosynthetic core gene clusters (BGCs) for secondary metabolite production identified in each species/strain. The counts of BGCs vary among the species/strains, whereby *G. lucidum* strain BCRC37177, *G. multipileum*, *G. lucidum* strain G260125-1, and *G. boninense* strain G3 have more than 30 putative BGCs. Most of the *Ganoderma* species/strains were found to have the highest counts for BGCs related to terpene biosynthesis followed by the BGCs for nonribosomal peptide synthase (NRPS)-like while only one BGC for NRPS was detected in each species/strain (except for *G. lucidum* strain BCRC37177 which has none). The *G. boninense* strain G3 was found to have a slightly higher number of BGCs associated with type 1 polyketide synthase (T1PKS) (Figure 2). The BGC for β-lactone production was identified in six *Ganoderma* species/strains but absent in *G. lucidum* strain G260125-1, *G. tsugae*, *G. boninense* strain NJ3, and *Ganoderma* sp. BRIUMSc. The BGC for clavaric acid production was identified as the most similar known cluster for terpene clusters in most *Ganoderma* species/strains except for *G. boninense* strain G3, *G. boninense* strain NJ3, *Ganoderma* sp. BRIUMSc, and *G. lucidum* strain BCRC36111. Meanwhile, the BGC for the biosynthesis of basidioferrin (an iron chelator) was identified as the most similar known cluster for NRPS/NRPS-like clusters in *G. lucidum* strain BCRC37177, *G. sinense,* and *Ganoderma* sp. BRIUMSc.
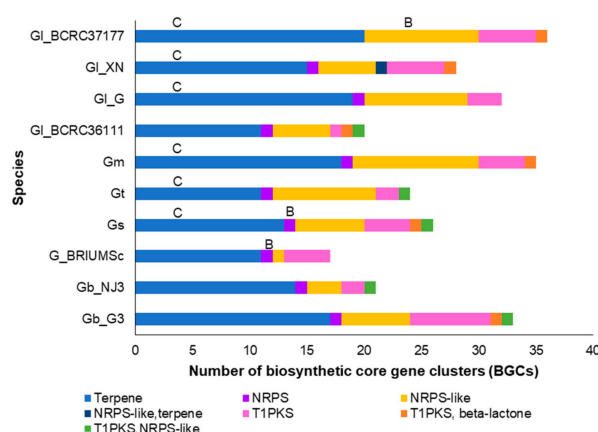
Figure 2. Counts of putative biosynthetic core gene clusters (BGCs) of *Ganoderma* species/strains identified by antiSMASH. The most similar known clusters were shown on top of the BGCs they belong: B, basidioferrin; and C, clavaric acid. Gb_G3, *G. boninense* strain G3; Gb_NJ3, *G. boninense* strain NJ3; Gm, *G. multipileum*; Gl_G, *G. lucidum* strain G260125-1; Gl_ BCRC36111, *G. lucidum* strain BCRC36111; Gl_BCRC37177, *G. lucidum* strain BCRC37177; Gl_XN, *G. lucidum* strain Xiangnong; Gs, *G. sinense*; Gt, *G. tsugae*; G_BRIUMSc, *Ganoderma* sp. BRIUMSc.

3.4. Identification of Ganoderma Orthologs

Since some of the predicted proteomes were of low quality, only the *Ganoderma* orthologs from seven *Ganoderma* proteomes which were more than 80% complete (Table 1) were further analyzed in this study. A total of 83,241 proteins were assigned to 14,238 ortholog clusters, with 6255 of them (50,153 proteins) shared by all seven *Ganoderma* species/strains whereas a total of 15,095 proteins were found in a single species/strain (singletons). A heatmap (similarity matrix of pairwise proteome comparisons) was plotted based on the ortholog clusters shared between a pair of proteomes (Figure 3A). *G. lucidum* strain BCRC37177 was found to share the highest number of ortholog clusters with *G. multipileum*.
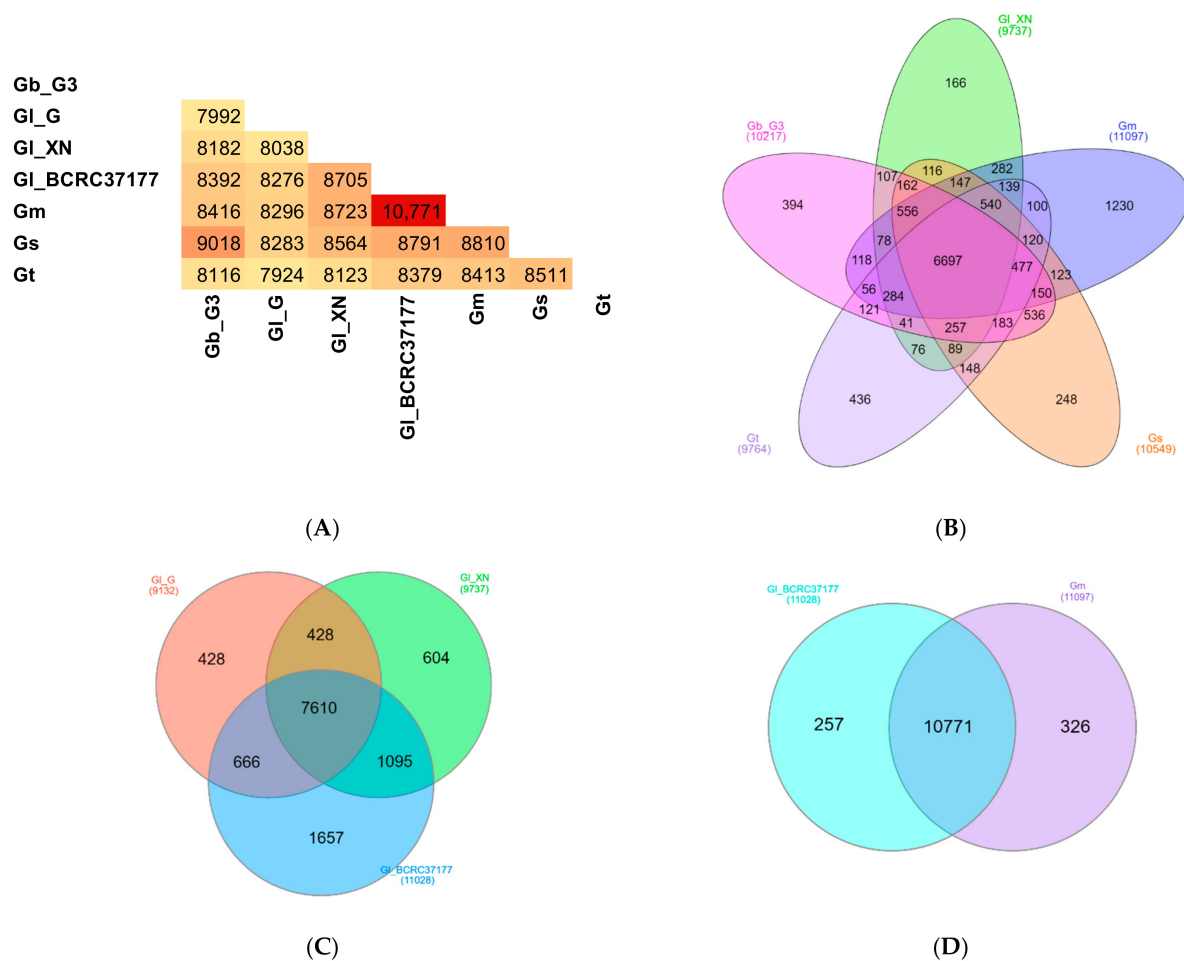

Figure 3. Pairwise proteome comparisons and Venn diagrams of ortholog clusters shared by *Ganoderma* species/strains. (**A**), similarity matrix of pairwise proteome comparisons. The numbers in the heat map show the number of ortholog clusters between a pair of proteomes; (**B**), the number of ortholog clusters shared by five representatives from different *Ganoderma* species; (**C**), the number of ortholog clusters shared by three *G. lucidum* strains; (**D**), the number of ortholog clusters shared by *G. lucidum* strain BCRC37177 and *G. multipileum*. Gb_G3, *G. boninense* strain G3; Gm, *G. multipileum*; Gl_G, *G. lucidum* strain G260125-1; Gl_ BCRC37177, *G. lucidum* strain BCRC37177; Gl_XN, *G. lucidum* strain Xiangnong; Gs, *G. sinense*; Gt, *G. tsugae*.

The numbers of orthologous groups shared by representatives of five different *Ganoderma* species, i.e., *G. boninense*, *G. lucidum*, *G. multipileum*, *G. sinense*, and *G. tsugae*, are shown in a Venn diagram in Figure 3B. *G. lucidum* strain Xiangnong was chosen as the representative for *G. lucidum* instead of *G. lucidum* strain BCRC37177, although the latter has a more complete proteome because *G. lucidum* strain BCRC37177 was found to share a higher

similarity with *G. multipileum* instead of other *G. lucidum* strains (Figure 3C). Figure 3B shows that 6697 clusters were shared by all five *Ganoderma* representative species, while the number of orthologous clusters shared by four, three, and two *Ganoderma* species were 2114, 1165, and 1727, respectively. A total of 2474 orthologous groups consisted of proteins from a single *Ganoderma* species (with the highest number of singletons in *G. multipileum*). Comparison of orthologous groups of the three *G. lucidum* strains (Figure 3C) revealed that 7610 orthologous groups were shared by all strains. The number of unique orthologous clusters which was only found in the proteome of a single *Ganoderma* species was 2689, mainly from *G. lucidum* strain BCRC37177. *G. lucidum* strain BCRC37177 shares the highest number of ortholog clusters with *G. multipileum* (previously mistaken as a tropical *G. lucidum*; [50]). A total of 10,771 orthologous groups were shared between *G. lucidum* strain BCRC37177 and *G. multipileum* (Figure 3D). Since the nomenclature of *Ganoderma* is confusing and no consensus has been achieved [5], it is possible that either of these *Ganoderma* spp. was incorrectly named.

3.5. Ganoderma Orthologous Groups Associated with Pathogenesis

The current study focuses on the ortholog groups with GO IDs related to biological and molecular functions that could possibly contribute to fungal virulence in plant-pathogenesis. A total of 98 ortholog clusters with GOs related to pathogenesis including mycotoxin biosynthesis, siderophore biosynthesis, transcription factors, transporter, fungal development, cell wall degradation, and others were found. Some of these ortholog groups are shown in Table 2.

Table 2. Selected ortholog groups related to pathogenesis assigned by OrthoVenn.

GO IDs	GO Annotation	Putative Identity of Protein	Number of Ortholog Group(s)	Number of Proteins	No Proteins in Each *Ganoderma* Species/Strains						
					Gb_G3	Gl_G	Gl_XN	Gl_BCRC37177	Gm	Gs	Gt
Mycotoxin metabolism											
GO:0009407	P:toxin catabolic process	Glutathione S-transferase U9	1	6	1	0	1	1	1	1	1
		Glutathione S-transferase U6	1	8	1	1	1	1	2	1	1
		Glutathione S-transferase U23	1	6	1	0	1	1	1	1	1
GO:0043386	P:mycotoxin biosynthetic process	Oxidase ustYa	2	12	3	1	2	1	1	2	2
GO:0045122	P:aflatoxin biosynthetic process	Norsolorinic acid ketoreductase	1	2	0	0	0	1	1	0	0
		O-methylsterigmatocystin oxidoreductase	2	8	1	2	1	1	1	1	1
		FAD-binding monooxygenase aflW	2	7	1	1	1	1	1	1	1
Secondary metabolism											
GO:0009820	P:alkaloid metabolic process	Tryprostatin B 6-hydroxylase	4	25	6	3	3	3	3	5	2
		Probable inactive reductase easA	2	16	4	2	2	2	2	2	2
GO:0035835	P:indole alkaloid biosynthetic process	Chanoclavine-I aldehyde reductase fgaOx3	9	6	1	0	1	1	1	1	1
GO:0019748	P:secondary metabolic process	Dehydrogenase orsE	2	14	2	2	1	2	2	3	2
		Isoflavone reductase (IFR) homolog A622-like	1	10	2	2	2	1	1	1	1
GO:0016114	P:terpenoid biosynthetic process	Cytochrome P450 monooxygenase andK	4	17	4	2	2	2	2	3	2
		Cytochrome P450 monooxygenase mpaDE	6	28	3	3	4	4	4	5	5
		Cytochrome P450 monooxygenase yanC	3	18	2	2	2	2	2	6	2
		Δ (6)-protoilludene synthase	10	60	10	10	5	10	9	9	7
		FAD-dependent monooxygenase yanF	3	6	0	0	0	0	2	0	4
		Methyltransferase ausD	2	6	0	1	0	1	2	1	1
		Methyltransferase trt5	1	6	1	1	1	0	0	2	1
		Multifunctional cytochrome P450	1	9	2	0	1	1	2	2	1
		N-Methyltransferase vrtF	2	4	1	0	0	1	1	1	0
		O-Mevalon transferase yanI	2	6	1	0	1	1	1	1	1

GO IDs	GO Annotation	Putative Identity of Protein	Number of Ortholog Group(s)	Number of Proteins	No Proteins in Each *Ganoderma* Species/Strains						
					Gb_G3	Gl_G	Gl_XN	Gl_BCRC37177	Gm	Gs	Gt
Pathogenesis											
GO:0009405	P:pathogenesis	Acyl-CoA ligase sidI	1	7	1	1	1	1	1	1	1
		Aldo-keto reductase AFTS1	5	17	3	3	1	2	3	3	2
		Cytochrome P450 monooxygenase BOA3	1	2	2	0	0	0	0	0	0
		Cytochrome P450 monooxygenase BOA4	3	16	2	3	2	3	2	2	2
		Cytochrome P450 monooxygenase CLM2	5	22	3	2	4	3	3	3	4
		Enoyl-CoA hydratase AFT3-1	3	21	1	3	3	3	3	4	4
		Enoyl-CoA isomerase/hydratase fer4	1	8	2	1	1	1	1	1	1
		FAD-dependent monooxygenase OpS4	8	44	4	6	6	8	8	7	5
		Hydroxymethylglutaryl (HMG)-CoA synthase	1	7	1	1	1	1	1	1	1
		Longiborneol synthase CLM1	7	39	6	3	7	8	7	5	3
		Orsellinic acid synthase ArmB	1	9	3	1	1	1	1	1	1
		Oxidoreductase BOA17	8	41	10	5	4	6	6	6	4
		Reducing polyketide synthase BOA9	1	5	0	0	1	1	1	1	1
		Fe-regulated protein 8	2	8	1	1	1	1	1	1	2
		Ferric/cupric reductase transmembrane	1	7	1	1	1	1	1	1	1
		β-1,2-xylosyltransferase 1	1	8	2	1	1	1	1	1	1
		bZIP transcription factor hapX	1	7	1	1	1	1	1	1	1
		C2H2 finger domain transcription factor dvrA	1	8	2	1	1	1	1	1	1
		Calcineurin subunit B	1	7	1	1	1	1	1	1	1
		Global transcription regulator sge1	1	7	1	1	1	1	1	1	1
		Glycerophosphoinositol permease 1	1	10	2	1	1	1	1	2	2
		LysM domain-containing protein ARB_00327	1	7	2	1	1	1	1	1	0
		Metallocarboxypeptidase A-like protein	1	10	1	2	1	1	2	2	1
		Probable aspartic-type endopeptidase CTSD	1	8	2	1	1	1	1	1	1
		Leucine aminopeptidase	2	19	3	3	2	2	2	3	4
		Tripeptidyl-peptidase SED2	7	34	5	4	7	4	4	4	6
		Tripeptidyl-peptidase SED3	2	15	2	3	2	2	2	2	2
		Tripeptidyl-peptidase SED4	2	8	3	1	1	1	1	1	0
Sterol biosynthesis and transport											
GO:0006696	P:ergosterol biosynthetic process	3-keto-steroid reductase (EC 1.1.1.270)	4	18	3	2	1	1	5	3	3
		C-8 sterol isomerase (EC 5.-.-.-)	1	7	1	1	1	1	1	1	1
		Ergosterol biosynthetic protein 28	1	7	1	1	1	1	1	1	1
		NADH-cytochrome b5 reductase 2 (EC 1.6.2.2)	1	7	1	1	1	1	1	1	1
		NADPH-cytochrome P450 reductase (EC 1.6.2.4)	1	7	1	1	1	1	1	1	1
		Sterol 24-C-methyltransferase erg6 (EC 2.1.1.-)	1	7	1	1	1	1	1	1	1
		Sterol-4-α-carboxylate 3-dehydrogenase (EC 1.1.1.170)	1	7	1	1	1	1	1	1	1
GO:0032443	P:regulation of ergosterol biosynthetic process	Damage response protein 1	1	7	1	1	1	1	1	1	1
GO:0015248	F:sterol transporter activity	Oxysterol-binding protein-related protein 3 (ORP-3)	1	7	1	1	1	1	1	1	1
		Protein PRY2 (Pathogenesis-related protein 2)	6	43	8	6	5	5	5	8	6
		Cell wall protein PRY3 (Pathogenesis-related protein 3)	2	12	1	2	2	2	2	2	1
Cell wall degradation											
GO:0046274	P: lignin catabolic process	3-O-methyltransferase	2	10	1	2	1	2	2	1	1
		4-O-methyl-glucuronoyl methylesterase	6	40	7	6	5	5	5	6	6
		4-O-methyltransferase	13	60	11	5	5	10	11	10	8
		Laccase	24	103	15	14	14	16	16	16	12
GO:0006979	P:response to oxidative stress	Ligninases	3	16	3	2	2	2	2	2	3
		Manganese peroxidase	3	19	4	2	2	2	2	4	3
		Versatile peroxidase	3	19	3	3	3	3	3	3	1

3.5.1. Mycotoxin and Secondary Metabolite Biosynthesis

A total of 35 ortholog clusters related to terpenoid biosynthetic process were discovered, including many polyketide synthases, cytochrome P450 monooxygenases, FAD-dependent monooxygenase, oxidoreductases, methyltransferases, and dehydrogenases (Table 2). Based on a homology search, some of them were possibly involved in the biosynthesis of mycotoxins such as yanuthone D, melleolides, culmorin, botcinic acid and botcinin derivatives terretonin, and mycophenolic acid, etc. In addition, *Ganoderma* orthologs related to alkaloid metabolism were identified. The orthologs for isoflavone reductase (IFR) homolog A622-like (a putative NADPH-dependent oxidoreductase involved in the biosynthesis of tobacco alkaloids; [51]) and chanoclavine-I aldehyde reductase (one of the enzymes which mediate the biosynthesis of a fungal ergot alkaloids known as isofumigaclavines; [52]) were also found in the *Ganoderma* species (Table 2).

Among the *Ganoderma* orthologs related to peptide mycotoxin biosynthesis, putative enzymes involved in the biosynthesis of AF-toxins e.g., aldo-keto reductase AFTS1, and enoyl-CoA hydratase AFT3-1 were identified. The *Ganoderma* orthologous implicated in the biosynthesis of aflatoxin and other mycotoxins (e.g.; ustiloxin B, gliotoxin and bibenzoquinone oosporein) include norsolorinic acid ketoreductase, O-methylsterigmatocystin oxidoreductase, FAD-binding monooxygenase aflW, and O-methylsterigmatocystin oxidoreductase, oxidase ustYa, cytochrome P450 monooxygenase gliF, and FAD-dependent monooxygenase and hydroxylase OpS4. In addition, there are orthologs for glutathione S-transferases which were possibly involved in toxin catabolic process. Several *Ganoderma* orthologs related to the biosynthesis of siderophore ferrichrome A, such as hydroxymethylglutaryl (HMG)-CoA synthase, enoyl-CoA isomerase/hydratase fer4, Fe-regulated protein 8, and acyl-CoA ligase sidI [53–55], were also identified (Table 2).

3.5.2. Ergosterol Biosynthesis and Sterol Transport

Ortholog clusters related to ergosterol biosynthesis (e.g., 3-keto-steroid reductases, C-8 sterol isomerase, ergosterol biosynthetic protein 28, NADH-cytochrome b5 reductase, sterol 24-C-methyltransferase, sterol-4-α-carboxylate 3-dehydrogenase) and regulation of ergosterol biosynthetic process (damage response protein 1) were also identified (Table 2). In addition, protein clusters related to sterol transport such as oxysterol-binding protein, pathogen related in yeast (PRY)2, PRY3, phosphatidylglycerol/phosphatidylinositol transfer protein and non-specific lipid-transfer protein (sterol carrier protein 2) were also identified in the *Ganoderma* species.

3.5.3. Other Virulence Factors

The orthologs for transcription factors related to plant-pathogenesis in *Ganoderma* species include global transcription regulator sge1 [56], bZIP transcription factor hapX [57], and C2H2 finger domain transcription factor dvrA [58]. Other orthologs related to virulence in *Ganoderma* species include calcineurin subunit B [59], LysM domain-containing protein ARB_00327 [60], extracellular metalloproteinase, metallocarboxypeptidase A-like protein, aspartic-type endopeptidase, leucine aminopeptidase, tripeptidyl-peptidases [61], which play different roles in fungal virulence (Table 2).

3.5.4. Lignolytic Enzymes and Other Plant-Cell-Wall Degrading Enzymes

Many ortholog clusters related to lignin catabolic process, including 3-O-methyltransferases, 4-O-methyl-glucuronoyl methylesterases, 4-O-methyltransferases, and laccases that may play a role in modifying or degrading plant lignin, were found in *Ganoderma* species. The seven *Ganoderma* species were found to have 103 laccases in total (Table 2). Peroxidases including 16 lignin peroxidases, 19 manganese peroxidase, and 19 versatile peroxidases were found among the ortholog groups related to stresses from *Ganoderma* species. In addition, ortholog clusters related to pectin biosynthetic process, pectin catabolic process, and cellulose catabolic process were also found among the *Ganoderma* species.

3.6. Putative Effectors from Ganoderma Species

In this study, only proteins with a signal peptide (normally 20–30 amino acid residue in length and positively charged, followed by a hydrophobic region and a cleavage site) were used as inputs for EffectorP analysis because signal peptides were expected to be important for the secretion of effectors for plant infection. The predicted effector proteins ranged from 0.85%–0.98% of each proteome, with the lowest percentage in *G. boninense* strain G3 and the highest percentage in *G. lucidum* strain BCRC37177 (Table 3). The predicted effectors with functional annotation ranged from 45.7%–59.0%. Among these effectors were allergens (such as Asp F7 and Asp F15), thaumatin-like proteins, PRY2, hydrophobins, papain inhibitor, ustiloxin B biosynthesis protein UstYa, etc. The GO:0005576 (extracellular region) was found to be overrepresented among the GOs of the predicted effectors from four *Ganoderma* species (i.e., *G. boninense* strain G3, *G. lucidum* strain BCRC37177, *G. sinense* ZZ0214-1 and *G. tsugae*), while GO:0005615 (extracellular space) was found to be overrepresented among the GOs of the predicted effectors of *G. lucidum* BCRC37177. Other GO terms that were overrepresented among the GOs of the predicted effectors include GO:0016798 (hydrolase activity acting on glycosyl bonds; in *G. tsugae*), GO:0010466 (negative regulation of peptidase activity; in *G. lucidum* strain G260125-1 and *G. multipileum*), and GO:0004867 (serine-type endopeptidase inhibitor activity; in *G. lucidum* strain G260125-1 and *G. multipileum*). No GO terms were over-represented among the predicted effectors of *G. lucidum* Xiangnong (Table 3).

Table 3. The number of putative effectors from *Ganoderma* Species.

	Number of Proteins with Signal Peptide	Number of Predicted Effector Proteins (% of Number of Proteins with Signal Peptide)	Number of Predicted Effector Proteins with Annotation	Over-Represented GO Terms of Effectors
G. boninense G3	2327	175 (7.5)	80	GO:0005576 (extracellular region) GO:0010466 (negative regulation of peptidase activity)
G. lucidum G260125-1	1407	102 (7.2)	59	GO:0004867 (serine-type endopeptidase inhibitor activity) GO:0043086 (negative regulation of catalytic activity)
G. lucidum Xiangnong	1565	107 (6.8)	52	-
G. lucidum BCRC37177	1592	123 (7.7)	66	GO:0005576 (extracellular region) GO:0005615 (extracellular space) GO:0010466 (negative regulation of peptidase activity)
G. multipileum	1625	118 (7.3)	63	GO:0004867 (serine-type endopeptidase inhibitor activity)
G. sinense ZZ0214-1	1908	153 (8.0)	71	GO:0005576 (extracellular region)
G. tsugae	1648	144 (8.7)	85	GO:0005576 (extracellular region) GO:0030234 (enzyme regulator activity) GO:0016798 (hydrolase activity, acting on glycosyl bonds)

The predicted effectors of *Ganoderma* species/strains were grouped into ortholog groups whereby 10 effector ortholog clusters were shared by six *Ganoderma* species/strains (Figure 4A), including papain inhibitor and thaumatin-like protein. About 21.7% of these ortholog groups (68 from a total of 313 groups) were conserved in at least four *Ganoderma* species/strains. Meanwhile, there are also putative effectors that are unique to only a single species (Figure 4A). Among the 175 predicted effectors from *G. boninense* strain G3, 111 (63.5%) of them were not found in other *Ganoderma* species. Figure 4B–D shows the distribution of the unique effectors from *G. boninense* strain G3 in different GO categories. Meanwhile, 72 of the predicted effectors from *G. boninense* strain G3 were found to be present in the transcriptome oil palm infected by *G. boninense* PER71 [20], including papain

inhibitor, allergen Asp F15, thaumatin-like protein 3.5 (allergen Cry j 3.5), protein PRY2, cytochrome P450 monooxygenase FSL4 (Fusarielin biosynthesis cluster protein 4), probable glycosidase C21B10.07 (EC 3.2.1.-), hydrophobin SC1, hydrophobin-1, etc. However, only 35 of these 72 predicted effectors were found to be unique to *G. boninense* strain G3 (not found in other *Ganoderma* species analyzed) (Figure 5). Almost all of these candidate effectors were found to be present only in oil palm roots treated with *G. boninense* PER71 but not in oil palm root sample treated with *Trichoderma*.

(**A**)

(**B**)

(**C**)

(**D**)
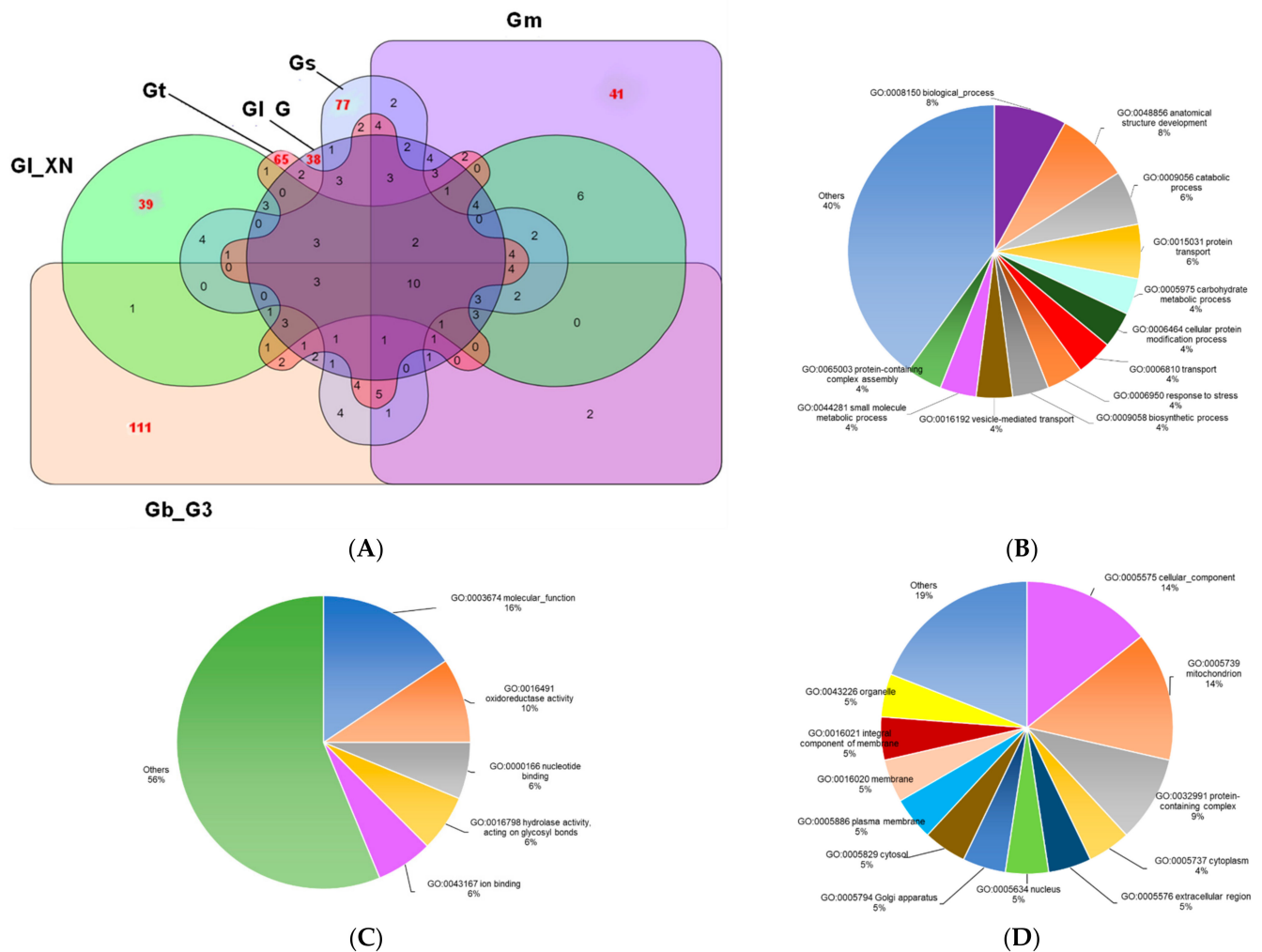
Figure 4. Predicted effectors in *Ganoderma* species/strains. (**A**), Venn diagram of effector orthologs of shared by *Ganoderma* species/strains. The numbers in black show the number of ortholog clusters shared by at least two *Ganoderma* species/strains while the numbers in red show the number of effectors that are unique to individual *Ganoderma* species/strains. Gb_G3, *G. boninense* strain G3; Gm, *G. multipileum*; Gl_G, *G. lucidum* strain G260125-1; Gl_XN, *G. lucidum* strain Xiangnong; Gs, *G. sinense*; Gt, *G. tsugae*. (**B**–**D**), GO classification of effectors that are unique to Gb_G3 in biological process (BP), molecular function (MF) and cellular component (CC), respectively.

Putative identity of effcetor	Gene expression, Log₂(RKPM)	
	G	T
Fruiting body protein SC1	14.19	7.75
Hydrophobin-1	11.68	
UPF0357 protein C1687.07	9.92	
Probable glycosidase C21B10.07	8.83	
FK506-binding protein 2	7.66	
Protein rot1	7.55	
Cytochrome b2	7.39	
Papain inhibitor	7.07	
Guanine nucleotide-binding protein alpha-4 subunit	7.05	
NADH-ubiquinone oxidoreductase 24 kDa subunit	6.75	
Protein priA	6.70	
ATP synthase subunit 5	6.60	
Uncharacterized membrane protein C17A5.08	6.45	
Long chronological lifespan protein 2	6.43	
Increased recombination centers protein 22-2	6.34	
Synaptobrevin homolog YKT6	5.63	
Thaumatin-like protein 1	5.47	
Presequence translocated-associated motor subunit PAM17	5.41	
Thaumatin-like protein	5.05	
Thioredoxin-like protein AAED1	4.87	
Increased recombination centers protein 22	4.49	
DnaJ-related protein spj1	4.42	
Probable coatomer subunit zeta	4.32	
Protein PRY2	4.28	
Probable arabinogalactan endo-beta-1	4.27	
Allergen Asp f 15	4.25	
Guanyl-specific ribonuclease Po1	4.11	
Protein phosphatase methylesterase 1	4.03	
Probable pyridoxal 5'-phosphate synthase subunit PDX2	4.02	
Deoxyuridine 5'-triphosphate nucleotidohydrolase	4.00	
Cytochrome P450 734A1	3.83	
Mitochondrial import inner membrane translocase subunit TIM22	3.71	
Probable N-acetylglucosaminyl-phosphatidylinositol de-N-acetylase	3.20	
Endoplasmic reticulum vesicle protein 25	3.16	
Uncharacterized J domain-containing protein C2E1P5.03	3.00	

Figure 5. Heat map displaying the differential expression of 35 unique effector genes in *G. boninense* strain G3. The differential expression levels (in Log₂[RKPM]) were calculated from the RPKM values of *Ganoderma* (G)- and *Trichoderma* (T)-inoculated oil palm root samples relative to that of untreated oil palm root sample (derived from the RNAseq data deposited at European Nucleotide Archive (ENA) under accession number: PRJEB7252). Red shows up-regulation whereby the fold change is represented by the number and color intensity (from low to high) while black indicates no expression.

4. Discussion

Ganoderma species are known to be either saprophytes that degrade dead wood or hemibiotrophs that cause stem, butt, and root rot in living trees [14]. All the *Ganoderma* species/strains analyzed in this study were predicted to be saprophytes except for *G. boninense* strain G3, which was predicted to be a hemibiotroph, and *G. lucidum* strain BCRC36111, which was predicted to be a symbiont, according to their CAZyme contents. *G. boninense* is a known pathogen which causes basal stem rot in oil palms [2]. Although *G. boninense* strain G3 was predicted to be a hemibiotroph as expected, the *G. boninense* strain NJ3 was classified as a saprophyte by CATAStrophy. This could possibly be due to the inferior quality of proteome from *G. boninense* strain NJ3. *G. lucidum* was generally found to be non-invasive to oil palms [62]. Although *G. lucidum*, *G. boninense,* and a few other *Ganoderma* species have been previously implicated as pathogens associated with stem rot in coconut [3], Vinjusha and Arun Kumar [63] revised the *Ganoderma* species associated with stem rot in coconut palms as *G. keralense* and *G. pseudoapplanatum*. Meanwhile, the ability of other *Ganoderma* species analyzed in this study to infect living trees was not clear. The presence and absence of certain groups of CAZymes were possibly important in determining the host plant specificity of a *Ganoderma* species/strain or in the determination of its trophic lifestyle. *G. boninense* strain G3, which was predicted to have a hemibiotrophic lifestyle, was found to have a higher number of GHs and GTs compared to other *Ganoderma* species or *G. bonienese* strain NJ3.

Ganoderma species are white rot fungi that can degrade lignin; hence, it is logical that cellulose-, lignin-, xylan-, and chitin-degrading enzymes were found to be widespread in the *Ganoderma* species/strains. The same groups of CAZymes were also reported by Sun et al. [13] in their study on the CAZymes from seven *Ganoderma* species, including

G. australe, G. leucocontextum, and *G. lingzhi,* which were not analyzed in this study. The *Ganoderma* species/strains were found to have a greater number of laccases than lignin peroxidases, manganese peroxidases, and versatile peroxidases. In addition, *Ganoderma* species/strains were also found to be rich in lytic polysaccharide monooxygenases, especially aryl alcohol oxidase, glucose 1-oxidase, copper-dependent lytic polysaccharide monooxygenases, gluco- or chito- oligosaccharide oxidases, and cellooligosaccharide dehydrogenases. These polysaccharide depolymerases may facilitate degradation of polysaccharides in plant cell walls. The ligninolytic enzymes and polysaccharide depolymerases are useful for the decomposition of wood, recycling of carbon, and lignin degradation for bioethanol production [64]. Pathogenic *Ganoderma* species may also use some of these CAZymes to degrade and modify plant cell walls during plant infection.

Ganoderma species were found to have a high content of biosynthetic core gene clusters associated with terpene biosynthesis and nonribosomal peptide synthase (NRPS)-like genes, in agreement with the findings of Jiang et al. [11] on the genomes of *G. tsugae, G. lingzhi, G. sinense,* and *G. boninense.* Most *Ganoderma* species/strains have the biosynthetic core gene for clavaric acid (a triterpenoid) except for *G. boninense* strain G3, *G. boninense* strain NJ3, and *Ganoderma* sp. BRIUMSc. Clavaric acid is found to be a potent inhibitor of the RAS farnesyltransferase, which plays a crucial role in the proliferation of tumor cells [65]. Its role in plant-pathogenesis has not been reported. The enzymes that participate in terpenoid biosynthesis were found to be present in all *Ganoderma* species/strains. Some of these proteins displayed high sequence similarities to enzymes in the biosynthesis of mycotoxins. Mycotoxins not only cause disease and death in the vertebrates that consume contaminated agricultural products [66] but may also be phytotoxic and play a role in plant pathogenesis [67,68]. In addition to terpenoids, peptide and ergot alkaloids form a large family of mycotoxins that consist of amino acid and isoprenoid precursors [66]. *Ganoderma* species were also found to have enzymes that are involved in the biosynthesis of AF-toxins, ustiloxin B, gliotoxin, bibenzoquinone oosporein, tryprostatins, ergovaline, and fumiclavanine C. The biosynthesis of basidioferrin siderophore is known to be catalyzed by an NRPS [69]. The gene cluster associated with the biosynthesis of basidioferrin was identified among the NRPS-like BGCs of *G. lucidum* strain BCRC37177 and *G. sinense* as well as the NRPS cluster of *Ganoderma* sp. BRIUMSc. However, all the *Ganoderma* species analyzed in this study were found to have a complete suite of enzymes in the biosynthesis of siderophore ferrichrome A, which contributes to organismal virulence. It is noteworthy that the gene expression of a *NRPS* gene of *G. boninense* strain UPMGB001 (belonging to the type VI siderophore-synthesizing NRPS family) was previously reported to be related to the basal stem rot disease severity of oil palm [70]. In addition, the bZIP transcription factor hapX, which represses genes related to iron-dependent and mitochondrial-localized activities during iron starvation [57], was identified in all *Ganoderma* species/strains. This transcription factor is critical for the coordination of the production of siderophores and their precursor ornithine [57] to ensure efficient iron uptake and inhibition of iron-consuming pathways [71]. Yasmin et al. [55] demonstrated that the interdependency of ergosterol and siderophore biosynthesis in *Aspergillus fumigatus* was governed by mevalonate (which is required for both biosynthetic pathways) through the acyl-CoA ligase SidI and the enoyl-CoA hydratase SidH. Iron-starvation induced the production of siderophore and decreased the ergosterol content and composition, which are critical for virulence. The biosynthetic core gene for β-lactone was identified in six of the *Ganoderma* species/strains analyzed in this study. It is a potent antibacterial and antifungal compound [72] which has been reported to inhibit the growth of fungi. β-lactone interferes with the biosynthesis of ergosterol by down-regulating the expression of HMG-CoA synthase [73]. The significance of bassidioferrin and β-lactone to the fungal virulence is unknown.

A few enzymes in the ergosterol biosynthesis pathway have been reported to be essential for fungal viability [74–77], vegetative differentiation, and virulence [78]. Ortholog clusters related to ergosterol biosynthesis and sterol transport were present in all the *Ganoderma* species/strains analyzed. The PRYs are sterol-binding and -export proteins

belonging to the CAP (cysteine-rich secretory protein, antigen 5, and pathogenesis-related 1) protein family [79]. Fungal pathogens sequester sterol from the host tissue through PRYs, which facilitate tissue penetration [79]. The PRY2 proteins are secreted glycoproteins while the PRY3 proteins are known to attach to glycosylphosphatidylinositol at the fungal cell wall [80,81]. PRY2 can export acetylated cholesterol [82] and was found to be hypersensitive to plant eugenol oil [81]. Although pathogen-specific PRYs may display distinct ligand-binding properties and/or protein stabilities [79], it is difficult to predict the pathogenicity of these putative PRYs solely based on the number of conserved cysteine residues involved in intramolecular disulfide bridges without evidence from laboratory experiments. Nevertheless, one of the PRY2 orthologs from *G. boninense* strain G3 was found to be highly similar to a sequence from *G. boninense* PER71, which was found to be expressed during oil palm root infection [20].

The infection mechanisms shared by the *Ganoderma* species/strains with other fungal pathogens can be inferred from the presence of annotated pathogenesis-related protein orthologs in their proteomes. The fungal infection process extends from germination or multiplication of an infective apparatus at the infection site to the establishment of a biotrophic or necrotrophic relationship with its host [83]. The proteins involved may include the global transcriptional regulator sge1, which participates in conidiogenesis and regulates the expression of fungal effectors during infection [56], and the C2H2 finger domain transcription factor dvrA, which may participate in the interactions between pathogen and host and regulate virulence negatively by changing the damaging capacity of a pathogen to host cells [58]. In addition, proteases (such as extracellular metalloproteinase, metallocarboxypeptidase A-like protein, aspartic-type endopeptidase, leucine aminopeptidase, and tripeptidyl-peptidases proteases) may facilitate the degradation of host proteins by these *Ganoderma* species/strains [61], while calcineurin subunit B (a calcium-dependent, calmodulin stimulated protein phosphatase) could play a central role in virulence and antifungal drug action [59] in *Ganoderma* species/strains. The presence of a glycerophosphodiester transporter in *Ganoderma* species/strains may mediate the uptake of glycerophosphoinositol as a source of inositol and phosphate [84,85] and expand the ability of fungi to utilize glycerophosphoinositol, hence enabling them to occupy a variety of environments within their host organisms [84]. Meanwhile, the LysM domain-containing protein ARB_00327 might protect the fungal hyphae from plant chitinases [86] and suppress host defenses by sequestering chitin oligosaccharides that trigger host immunity [60].

The current study predicted and compared putative fungal effectors from different *Ganoderma* species/strains including species that are pathogenic and non-pathogenic to oil palms. The approach herein is different from the approach employed by Khairi et al. [37], who predicted effector proteins from the pan genomes of *G. boninense*. Few predicted effectors were conserved in all seven species, and many putative effectors are unique to only one *Ganoderma* species/strain. These putative effectors are possibly responsible for host specificity and specific host–pathogen interactions. About 41% of the predicted effectors from *G. boninense* strain G3 were found to be expressed in *G. boninense* PER71 during oil palm infection [20]. These groups of unique fungal effectors may have more potential to be associated with basal stem rot disease in oil palm. Some of these putative effectors were also found to be expressed *in planta* by a separate study [37] using different RNAseq datasets. Among these unique effectors are putative allergen Asp F15, thaumatin-like protein 1, PRY2, protein rot1, cytochrome P450 monooxygenase FSL4, cytochrome P450 734A, thioredoxin-like protein AAED1, and hydrophobin. Asp F15 is an allergen which belongs to the cerato-platanin family. The cerato-platanin protein could also be a phytotoxin which causes plant disease [87], and it was reported to induce cell necrosis and phytoalexin synthesis in plants [88]. Moreover, hydrophobin and thaumatin-like protein were reported to be involved in the development and senescence of the fruiting body, respectively [89,90]. In addition, thaumatin-like protein may have β-1,3-glucanase activities which can modify fungal cell walls [91]. Although fusarielins exhibit antibacterial, antifungal, anticancer, anti-angiogenic, and antiproliferative properties [92], the role of these polyketides in plant

pathogenesis is not clear. Since most of these candidate effectors were found to be present only in oil palm roots treated with *G. boninense* but not in oil palm root samples treated with *Trichoderma*, these candidate effectors could serve as targets for the development of antifungal agents that are specific to the pathogen. The roles of these candidate effectors in oil palm infection await further elucidation.

5. Conclusions

The comparative genomics analyses of the proteomes of *Ganoderma* species/strains in this study revealed that: 1. *G. boninense* is likely a hemibiotroph based on its CAZyme content (in support of its aggressiveness as a potent pathogen to oil palm) while all the other *Ganoderma* species/strains being analyzed were predicted to adopt a saprophytic or a symbiotic lifestyle; 2. *Ganoderma* species/strains shared many CAZymes and secondary metabolite core gene clusters, in line with their ability to degrade plant cell walls and to produce high values secondary metabolites; however, there are also unique CAZyme classes and secondary metabolite core genes that are unique in individual species; 3. Protein orthologs that are related to pathogenesis including those related to mycotoxin and secondary metabolite biosynthesis, ergosterol biosynthesis and transport, as well as virulence factors were identified for further functional experiments; 4. Potential effectors were also identified for *Ganoderma* species/strains, especially unique effectors that were expressed in *G. boninense* in oil palm roots, causing basal stem rot disease. These are useful resources for future analyses of the fungal pathogenesis of *Ganoderma* species.

Supplementary Materials: The following supporting information can be downloaded at: https://www.mdpi.com/article/10.3390/f14030653/s1, Table S1: Information of the Ganoderma species and genome assemblies.

Data Availability Statement: The datasets generated during the current study are available from the corresponding author on reasonable request.

Conflicts of Interest: The author declares no conflict of interest. The funders had no role in the design of the study; in the collection, analyses, or interpretation of data; in the writing of the manuscript; or in the decision to publish the results.

References

1. Baby, S.; Johnson, A.J.; Govindan, B. Secondary metabolites from *Ganoderma*. *Phytochem.* **2015**, *114*, 66–101. [CrossRef]
2. Mohammed, C.L.; Rimbawanto, A.; Page, D.E. Management of basidiomycete root- and stem-rot diseases in oil palm, rubber and tropical hardwood plantation crops. *For. Path.* **2014**, *44*, 428–446. [CrossRef]
3. Kandan, A.; Bhaskaran, R.; Samiyappan, R. *Ganoderma*—A basal stem rot disease of coconut palm in south Asia and Asia pacific regions. *Arch. Phytopathol. Pflanzenschutz.* **2010**, *43*, 1445–1449. [CrossRef]
4. Loyd, A.L.; Linder, E.R.; Anger, N.A.; Richter, B.S.; Blanchette, R.A.; Smith, J.A. Pathogenicity of *Ganoderma* species on landscape trees in the Southeastern United States. *Plant Dis.* **2018**, *102*, 1944–1949. [CrossRef]
5. Bishop, K.S.; Kao, C.H.; Xu, Y.; Glucina, M.P.; Paterson, R.R.; Ferguson, L.R. From 2000 years of *Ganoderma lucidum* to recent developments in nutraceuticals. *Phytochemistry* **2015**, *114*, 56–65. [CrossRef] [PubMed]
6. Ferreira, I.C.; Heleno, S.A.; Reis, F.S.; Stojkovic, D.; Queiroz, M.J.; Vasconcelos, M.H.; Sokovic, M. Chemical features of *Ganoderma* polysaccharides with antioxidant, antitumor and antimicrobial activities. *Phytochemistry* **2015**, *114*, 38–55. [CrossRef]
7. Peng, X.; Liu, J.; Xia, J.; Wang, C.; Li, X.; Deng, Y.; Bao, N.; Zhang, Z.; Qiu, M. Lanostane triterpenoids from *Ganoderma hainanense* J. D. Zhao. *Phytochemistry* **2015**, *114*, 137–145. [CrossRef] [PubMed]
8. Zhang, Y.; Jiang, Y.; Zhang, M.; Zhang, L. *Ganoderma sinense* polysaccharide: An adjunctive drug used for cancer treatment. *Prog. Mol. Biol. Transl. Sci.* **2019**, *163*, 165–177. [CrossRef] [PubMed]
9. Liang, C.; Tian, D.; Liu, Y.; Li, H.; Zhu, J.; Li, M.; Xin, M.; Xia, J. Review of the molecular mechanisms of *Ganoderma lucidum* triterpenoids: Ganoderic acids A, C2, D, F, DM, X and Y. *Eur. J. Med. Chem.* **2019**, *174*, 130–141. [CrossRef]
10. Pattanayak, S.; Das, S.; Biswal, G. Ganoderma: The wild mushroom with wonderful health benefits. *J. Pharmacogn. Phytochem.* **2020**, *9*, 313–316. [CrossRef]
11. Jiang, N.; Hu, S.; Peng, B.; Li, Z.; Yuan, X.; Xiao, S.; Fu, Y. Genome of *Ganoderma* species provides Insights Into the evolution, conifers substrate utilization, and terpene synthesis for *Ganoderma tsugae*. *Front. Microbiol.* **2021**, *12*, 724451. [CrossRef]

12. Tian, Y.Z.; Wang, Z.F.; Liu, Y.D.; Zhang, G.Z.; Li, G. The whole-genome sequencing and analysis of a *Ganoderma lucidum* strain provide insights into the genetic basis of its high triterpene content. *Genomics* **2021**, *113*, 840–849. [CrossRef] [PubMed]

13. Sun, Y.F.; Lebreton, A.; Xing, J.H.; Fang, Y.X.; Si, J.; Morin, E.; Miyauchi, S.; Drula, E.; Ahrendt, S.; Cobaugh, K.; et al. Phylogenomics and Comparative Genomics Highlight Specific Genetic Features in *Ganoderma* Species. *J. Fungi* **2022**, *8*, 311. [CrossRef] [PubMed]

14. Kües, U.; Nelson, D.R.; Liu, C.; Yu, G.J.; Zhang, J.; Li, J.; Wang, X.C.; Sun, H. Genome analysis of medicinal *Ganoderma* spp. with plant-pathogenic and saprotrophic life-styles. *Phytochemistry* **2015**, *114*, 18–37. [CrossRef]

15. Chen, S.; Xu, J.; Liu, C.; Zhu, Y.; Nelson, D.R.; Zhou, S.; Li, C.; Wang, L.; Guo, X.; Sun, Y.; et al. Genome sequence of the model medicinal mushroom *Ganoderma lucidum*. *Nat. Commun.* **2012**, *3*, 913. [CrossRef]

16. Yu, G.J.; Wang, M.; Huang, J.; Yin, Y.L.; Chen, Y.J.; Jiang, S.; Jin, Y.X.; Lan, X.Q.; Wong, B.H.; Liang, Y.; et al. Deep insight into the *Ganoderma lucidum* by comprehensive analysis of its transcriptome. *PLoS ONE* **2012**, *7*, e44031. [CrossRef]

17. Huang, Y.H.; Wu, H.Y.; Wu, K.M.; Liu, T.T.; Liou, R.F.; Tsai, S.F.; Shiao, M.S.; Ho, L.T.; Tzean, S.S.; Yang, U.C. Generation and analysis of the expressed sequence tags from the mycelium of *Ganoderma lucidum*. *PLoS ONE* **2013**, *8*, e61127. [CrossRef]

18. Ramzi, A.B.; Che Me, M.L.; Ruslan, U.S.; Baharum, S.N.; Nor Muhammad, N.A. Insight into plant cell wall degradation and pathogenesis of *Ganoderma boninense* via comparative genome analysis. *PeerJ* **2019**, *7*, e8065. [CrossRef]

19. Ho, P.Y.; Namasivayam, P.; Sundram, S.; Ho, C.L. Expression of genes encoding manganese peroxidase and laccase of *Ganoderma boninense* in response to nitrogen sources, hydrogen peroxide and phytohormones. *Genes* **2020**, *11*, 1263. [CrossRef]

20. Ho, C.L.; Tan, Y.C.; Yeoh, K.A.; Ghazali, A.K.; Yee, W.Y.; Hoh, C.C. *De novo* transcriptome analyses of host-fungal interactions in oil palm (*Elaeis guineensis* Jacq.). *BMC Genom.* **2016**, *17*, 66. [CrossRef]

21. Ko, E.M.; Leem, Y.E.; Choi, H.T. Purification and characterization of laccase isozymes from the white-rot basidiomycete *Ganoderma lucidum*. *Appl. Microbiol. Biotechnol.* **2001**, *57*, 98–102. [CrossRef] [PubMed]

22. Teerapatsakul, C.; Abe, N.; Bucke, C.; Chitradon, L. Novel laccases of *Ganoderma* sp. KU-Alk4, regulated by different glucose concentration in alkaline media. *World J. Microbiol. Biotechnol.* **2007**, *23*, 1559–1567. [CrossRef]

23. Kumar, A.; Kant, K.; Kumar., P.; Ramchiary., N. Laccase isozymes from *Ganoderma lucidum* MDU-7: Isolation, characterization, catalytic properties and differential role during oxidative stress. *J. Mol. Catal. Enzymat.* **2015**, *113*, 68–75. [CrossRef]

24. Torres-Farradá, G.; Manzano León, A.M.; Rineau, F.; Ledo Alonso, L.L.; Sánchez-López, M.I.; Thijs, S.; Colpaert, J.; Ramos-Leal, M.; Guerra, G.; Vangronsveld, J. Diversity of ligninolytic enzymes and their genes in strains of the genus *Ganoderma*: Applicable for biodegradation of xenobiotic compounds? *Front. Microbiol.* **2017**, *8*, 898. [CrossRef]

25. Si, J.; Wu, Y.; Ma, H.F.; Cao, Y.J.; Sun, Y.F.; Cui, B.K. Selection of a pH- and temperature-stable laccase from *Ganoderma australe* and its application for bioremediation of textile dyes. *J. Environ. Manag.* **2021**, *299*, 113619. [CrossRef] [PubMed]

26. Xu, H.; Guo, M.Y.; Gao, Y.H.; Bai, X.H.; Zhou, X.W. Expression and characteristics of manganese peroxidase from *Ganoderma lucidum* in *Pichia pastoris* and its application in the degradation of four dyes and phenol. *BMC Biotechnol.* **2017**, *17*, 19. [CrossRef]

27. Zhuo, R.; Ma, L.; Fan, F.; Gong, Y.; Wan, X.; Jiang, M.; Zhang, X.; Yang, Y. Decolorization of different dyes by a newly isolated white-rot fungi strain *Ganoderma* sp. En3 and cloning and functional analysis of its laccase gene. *J. Hazard. Mater.* **2011**, *192*, 855–873. [CrossRef]

28. You, L.F.; Liu, Z.M.; Lin, J.F.; Guo, L.Q.; Huang, X.L.; Yang, H.X. Molecular cloning of a laccase gene from *Ganoderma lucidum* and heterologous expression in *Pichia pastoris*. *J. Basic Microbiol.* **2014**, *54*, S134–S141. [CrossRef] [PubMed]

29. Wang, H.; Deng, W.; Shen, M.; Yan, G.; Zhao, W.; Yang, Y. A laccase Gl-LAC-4 purified from white-rot fungus *Ganoderma lucidum* had a strong ability to degrade and detoxify the alkylphenol pollutants 4-n-octylphenol and 2-phenylphenol. *J. Hazard. Mater.* **2021**, *408*, 124775. [CrossRef] [PubMed]

30. Teh, C.Y.; Pang, C.; Tor, X.Y.; Ho, P.; Lim, Y.; Namasivayam, P.; Ho, C.L. Molecular cloning and functional analysis of a necrosis and ethylene inducing protein (NEP) from *Ganoderma boninense*. *Physiol. Mol. Plant Pathol.* **2019**, *106*, 42–48. [CrossRef]

31. Lim, F.-H.; Fakhrana, I.N.; Rasid, O.A.; Idris, A.S.; Ho, C.-L.; Shaharuddin, N.A.; Parveez, G.K.A. Molecular cloning and expression analysis of *Ganoderma boninense* cyclophilins at different growth and infection stages. *Physiol. Mol. Plant Pathol.* **2017**, *99*, 31–40. [CrossRef]

32. Sulaiman, S.; Yusoff, N.; Tan, J.S.; Lee, Y.P. Deciphering the pan-genome of *Ganoderma* sp. to depict potential genomic components that contribute to *Ganoderma boninense* pathogenicity. *Malays. Appl. Biol.* **2018**, *47*, 71–80.

33. Zhu, Y.; Xu, J.; Sun, C.; Zhou, S.; Xu, H.; Nelson, D.R.; Qian, J.; Song, J.; Luo, H.; Xiang, L.; et al. Chromosome-level genome map provides insights into diverse defense mechanisms in the medicinal fungus *Ganoderma sinense*. *Sci. Rep.* **2015**, *5*, 11087. [CrossRef] [PubMed]

34. Liu, Y.; Huang, L.; Hu, H.; Cai, M.; Liang, X.; Li, X.; Zhang, Z.; Xie, Y.; Xiao, C.; Chen, S.; et al. Whole-genome assembly of *Ganoderma leucocontextum* (Ganodermataceae, Fungi) discovered from the Tibetan Plateau of China. *G3* **2021**, *11*, jkab337. [CrossRef] [PubMed]

35. Binder, M.; Justo, A.; Riley, R.; Salamov, A.; Lopez-Giraldez, F.; Sjökvist, E.; Copeland, A.; Foster, B.; Sun, H.; Larsson, E.; et al. Phylogenetic and phylogenomic overview of the Polyporales. *Mycologia* **2013**, *105*, 1350–1373. [CrossRef] [PubMed]

36. Liu, D.; Gong, J.; Dai, W.; Kang, X.; Huang, Z.; Zhang, H.M.; Liu, W.; Liu, L.; Ma, J.; Xia, Z.; et al. The genome of *Ganoderma lucidum* provides insights into triterpenes biosynthesis and wood degradation. *PLoS ONE* **2012**, *7*, e36146. [CrossRef]

37. Khairi, M.H.F.; Nor Muhammad, N.A.; Bunawan, H.; Abdul Murad, A.M.; Ramzi, A.B. Unveiling the core effector proteins of oil palm pathogen *Ganoderma boninense* via pan-secretome analysis. *J. Fungi* **2022**, *8*, 793. [CrossRef]

38. Seppey, M.; Manni, M.; Zdobnov, E.M. BUSCO: Assessing genome assembly and annotation completeness. *Methods Mol. Biol.* **2019**, *1962*, 227–245. [CrossRef]

39. Götz, S.; García-Gómez, J.M.; Terol, J.; Williams, T.D.; Nagaraj, S.H.; Nueda, M.J.; Robles, M.; Talón, M.; Dopazo, J.; Conesa, A. High-throughput functional annotation and data mining with the Blast2GO suite. *Nucleic Acids Res.* **2008**, *36*, 3420–3435. [CrossRef]

40. Kanehisa, M.; Sato, Y.; Morishima, K. BlastKOALA and GhostKOALA: KEGG tools for functional characterization of genome and metagenome sequences. *J. Mol. Biol.* **2016**, *428*, 726–731. [CrossRef]

41. Blin, K.; Shaw, S.; Kloosterman, A.M.; Charlop-Powers, Z.; van Wezel, G.P.; Medema, M.H.; Weber, T. antiSMASH 6.0: Improving cluster detection and comparison capabilities. *Nucleic Acids Res.* **2021**, *49*, W29–W35. [CrossRef]

42. Eddy, S.R. A new generation of homology search tools based on probabilistic inference. *Genome Inform.* **2009**, *23*, 205–211.

43. Yin, Y.; Mao, X.; Yang, J.; Chen, X.; Mao, F.; Xu, Y. dbCAN: A web resource for automated carbohydrate-active enzyme annotation. *Nucleic Acids Res.* **2012**, *40*, W445–W451. [CrossRef] [PubMed]

44. Hane, J.K.; Paxman, J.; Jones, D.A.B.; Oliver, R.P.; de Wit, P. "CATAStrophy", a genome-informed trophic classification of filamentous plant pathogens—How many different types of filamentous plant pathogens are there? *Front. Microbiol.* **2020**, *10*, 3088. [CrossRef] [PubMed]

45. Li, L.; Stoeckert, C.J., Jr.; Roos, D.S. OrthoMCL: Identification of ortholog groups for eukaryotic genomes. *Genome Res.* **2003**, *13*, 2178–2189. [CrossRef]

46. Xu, L.; Dong, Z.; Fang, L.; Luo, Y.; Wei, Z.; Guo, H.; Zhang, G.; Gu, Y.Q.; Coleman-Derr, D.; Xia, Q.; et al. OrthoVenn2: A web server for whole-genome comparison and annotation of orthologous clusters across multiple species. *Nucleic Acids Res.* **2019**, *47*, W52–W58. [CrossRef]

47. Heberle, H.; Meirelles, G.V.; da Silva, F.R.; Telles, G.P.; Minghim, R. InteractiVenn: A web-based tool for the analysis of sets through Venn diagrams. *BMC Bioinform.* **2015**, *16*, 169. [CrossRef] [PubMed]

48. Käll, L.; Krogh, A.; Sonnhammer, E.L. A combined transmembrane topology and signal peptide prediction method. *J. Mol. Biol.* **2004**, *338*, 1027–1036. [CrossRef] [PubMed]

49. Sperschneider, J.; Dodds, P.N.; Gardiner, D.M.; Singh, K.B.; Taylor, J.M. Improved prediction of fungal effector proteins from secretomes with EffectorP 2.0. *Mol. Plant Path.* **2018**, *19*, 2094–2110. [CrossRef]

50. Wang, D.; Wu, S.; Su, C.; Peng, J.; Shih, Y.; Chen, L. *Ganoderma multipileum*, the correct name for '*G. lucidum*' in tropical Asia. *Bot. Stud.* **2009**, *50*, 451–458.

51. Kajikawa, M.; Hirai, N.; Hashimoto, T. A PIP-family protein is required for biosynthesis of tobacco alkaloids. *Plant Mol. Biol.* **2009**, *69*, 287–298. [CrossRef] [PubMed]

52. Fernández-Bodega, Á.; Álvarez-Álvarez, R.; Liras, P.; Martín, J.F. Silencing of a second dimethylallyltryptophan synthase of *Penicillium roqueforti* reveals a novel clavine alkaloid gene cluster. *Appl. Microbiol. Biotechnol.* **2017**, *101*, 6111–6121. [CrossRef] [PubMed]

53. Eichhorn, H.; Lessing, F.; Winterberg, B.; Schirawski, J.; Kämper, J.; Müller, P.; Kahmann, R. A ferroxidation/permeation iron uptake system is required for virulence in *Ustilago maydis*. *Plant Cell* **2006**, *18*, 3332–3345. [CrossRef]

54. Winterberg, B.; Uhlmann, S.; Linne, U.; Lessing, F.; Marahiel, M.A.; Eichhorn, H.; Kahmann, R.; Schirawski, J. Elucidation of the complete ferrichrome A biosynthetic pathway in *Ustilago maydis*. *Mol. Microbiol.* **2010**, *75*, 1260–1271. [CrossRef]

55. Yasmin, S.; Alcazar-Fuoli, L.; Gründlinger, M.; Puempel, T.; Cairns, T.; Blatzer, M.; Lopez, J.F.; Grimalt, J.O.; Bignell, E.; Haas, H. Mevalonate governs interdependency of ergosterol and siderophore biosyntheses in the fungal pathogen *Aspergillus fumigatus*. *Proc. Natl. Acad. Sci. USA* **2012**, *109*, E497–E504. [CrossRef] [PubMed]

56. Michielse, C.B.; van Wijk, R.; Reijnen, L.; Manders, E.M.; Boas, S.; Olivain, C.; Alabouvette, C.; Rep, M. The nuclear protein Sge1 of *Fusarium oxysporum* is required for parasitic growth. *PLoS Pathog.* **2009**, *5*, e1000637. [CrossRef] [PubMed]

57. Liu, H.; Gravelat, F.N.; Chiang, L.Y.; Chen, D.; Vanier, G.; Ejzykowicz, D.E.; Ibrahim, A.S.; Nierman, W.C.; Sheppard, D.C.; Filler, S.G. *Aspergillus fumigatus* AcuM regulates both iron acquisition and gluconeogenesis. *Mol. Microbiol.* **2010**, *78*, 1038–1054. [CrossRef]

58. Ejzykowicz, D.E.; Solis, N.V.; Gravelat, F.N.; Chabot, J.; Li, X.; Sheppard, D.C.; Filler, S.G. Role of *Aspergillus fumigatus DvrA* in host cell interactions and virulence. *Eukaryot Cell* **2010**, *9*, 1432–1440. [CrossRef]

59. Fox, D.S.; Cruz, M.C.; Sia, R.A.; Ke, H.; Cox, G.M.; Cardenas, M.E.; Heitman, J. Calcineurin regulatory subunit is essential for virulence and mediates interactions with FKBP12-FK506 in *Cryptococcus neoformans*. *Mol. Microbiol.* **2001**, *39*, 835–849. [CrossRef]

60. De Jonge, R.; Thomma, B.P. Fungal LysM effectors: Extinguishers of host immunity? *Trends Microbiol.* **2009**, *17*, 151–157. [CrossRef]

61. Krishnan, P.; Ma, X.; McDonald, B.A.; Brunner, P.C. Widespread signatures of selection for secreted peptidases in a fungal plant pathogen. *BMC Evol. Biol.* **2018**, *18*, 7. [CrossRef] [PubMed]

62. Siddiqui, Y.; Surendran, A.; Paterson, R.R.M.; Ali, A.; Ahmad, K. Current strategies and perspectives in detection and control of basal stem rot of oil palm. *Saudi J. Biol.* **2021**, *28*, 2840–2849. [CrossRef] [PubMed]

63. Vinjusha, N.; Arun Kumar, T.K. Revision of *Ganoderma* species associated with stem rot of coconut palm. *Mycologia* **2022**, *114*, 157–174. [CrossRef] [PubMed]

64. Zhao, C.; Qiao, X.; Shao, Q.; Hassan, M.; Ma, Z. Evolution of the lignin chemical structure during the bioethanol production process and its inhibition to enzymatic hydrolysis. *Energy Fuels* **2020**, *34*, 5938–5947. [CrossRef]

65. Jayasuriya, H.; Silverman, K.C.; Zink, D.L.; Jenkins, R.G.; Sanchez, M.; Pelaez, F.; Vilella, D.; Lingham, R.B.; Singh, S.B. Clavaric acid: A triterpenoid inhibitor of farnesyl-protein transferase from *Clavariadelphus truncatus*. *J. Nat. Prod.* **1998**, *61*, 1568–1570. [CrossRef] [PubMed]

66. Desjardins, A.E.; Hohn, T.M. Mycotoxins in plant pathogenesis. *Mol. Plant Microbe Interact.* **1997**, *10*, 147–152. [CrossRef]

67. Panaccione, D.G.; Scott-Craig, J.S.; Pocard, J.A.; Walton, J.D. A cyclic peptide synthetase gene required for pathogenicity of the fungus *Cochliobolus carbonum* on maize. *Proc. Natl. Acad. Sci. USA* **1992**, *89*, 6590–6594. [CrossRef]

68. Baker, S.E.; Kroken, S.; Inderbitzin, P.; Asvarak, T.; Li, B.Y.; Shi, L.; Yoder, O.C.; Turgeon, B.G. Two polyketide synthase-encoding genes are required for biosynthesis of the polyketide virulence factor, T-toxin, by *Cochliobolus heterostrophus*. *Mol. Plant Microbe Interact.* **2006**, *19*, 139–149. [CrossRef] [PubMed]

69. Koczyk, G.; Pawłowska, J.; Muszewska, A. Terpenoid biosynthesis dominates among secondary metabolite clusters in *Mucoromycotina* genomes. *J. Fungi* **2021**, *7*, 285. [CrossRef] [PubMed]

70. Shokrollahi, N.; Ho, C.L.; Zainudin, N.A.I.M.; Wahab, M.A.B.A.; Wong, M.Y. Identification of non-ribosomal peptide synthetase in *Ganoderma boninense* Pat. that was expressed during the interaction with oil palm. *Sci. Rep.* **2021**, *11*, 16330. [CrossRef]

71. Kröber, A.; Scherlach, K.; Hortschansky, P.; Shelest, E.; Staib, P.; Kniemeyer, O.; Brakhage, A.A. HapX mediates iron homeostasis in the pathogenic dermatophyte *Arthroderma benhamiae* but is dispensable for virulence. *PLoS ONE* **2016**, *11*, e0150701. [CrossRef]

72. Robinson, S.L.; Christenson, J.K.; Wackett, L.P. Biosynthesis and chemical diversity of β-lactone natural products. *Nat. Prod. Rep.* **2019**, *36*, 458–475. [CrossRef] [PubMed]

73. Tang, X.X.; Yan, X.; Fu, W.H.; Yi, L.Q.; Tang, B.W.; Yu, L.B.; Fang, M.J.; Wu, Z.; Qiu, Y.K. New β-lactone with tea pathogenic fungus inhibitory effect from marine-derived fungus MCCC3A00957. *J. Agric. Food Chem.* **2019**, *67*, 2877–2885. [CrossRef] [PubMed]

74. Lees, N.D.; Skaggs, B.; Kirsch, D.R.; Bard, M. Cloning of the late genes in the ergosterol biosynthetic pathway of *Saccharomyces cerevisiae*—A review. *Lipids* **1995**, *30*, 221–226. [CrossRef] [PubMed]

75. Aaron, K.E.; Pierson, C.A.; Lees, N.D.; Bard, M. The *Candida albicans* ERG26 gene encoding the C-3 sterol dehydrogenase (C-4 decarboxylase) is essential for growth. *FEMS Yeast Res.* **2001**, *1*, 93–101. [CrossRef] [PubMed]

76. Kennedy, M.A.; Johnson, T.A.; Lees, N.D.; Barbuch, R.; Eckstein, J.A.; Bard, M. Cloning and sequencing of the *Candida albicans* C-4 sterol methyl oxidase gene (ERG25) and expression of an ERG25 conditional lethal mutation in *Saccharomyces cerevisiae*. *Lipids* **2000**, *35*, 257–262. [CrossRef]

77. Pierson, C.A.; Jia, N.; Mo, C.; Lees, N.D.; Sturm, A.M.; Eckstein, J.; Barbuct, R.; Bard, M. Isolation, characterization, and regulation of the *Candida albicans ERG27* gene encoding the sterol 3-keto reductase. *Med. Mycol.* **2004**, *42*, 461–473. [CrossRef]

78. Liu, Z.; Jian, Y.; Chen, Y.; Kistler, H.C.; He, P.; Ma, Z.; Yin, Y. A phosphorylated transcription factor regulates sterol biosynthesis in *Fusarium graminearum*. *Nat. Commun.* **2019**, *10*, 1228. [CrossRef]

79. Schneiter, R.; Di Pietro, A. The CAP protein superfamily: Function in sterol export and fungal virulence. *Biomol. Concepts* **2013**, *4*, 519–525. [CrossRef]

80. Yin, Q.Y.; de Groot, P.W.; Dekker, H.L.; de Jong, L.; Klis, F.M.; de Koster, C.G. Comprehensive proteomic analysis of *Saccharomyces cerevisiae* cell walls: Identification of proteins covalently attached via glycosylphosphatidylinositol remnants or mild alkali-sensitive linkages. *J. Biol. Chem.* **2005**, *280*, 20894–20901. [CrossRef]

81. Choudhary, V.; Schneiter, R. Pathogen-Related Yeast (PRY) proteins and members of the CAP superfamily are secreted sterol-binding proteins. *Proc. Natl. Acad. Sci. USA* **2012**, *109*, 16882–16887. [CrossRef] [PubMed]

82. Tiwari, R.; Köffel, R.; Schneiter, R. An acetylation/deacetylation cycle controls the export of sterols and steroids from *S. cerevisiae*. *EMBO J.* **2007**, *26*, 5109–5119. [CrossRef] [PubMed]

83. Ravichandra, N.G. *Frontiers in Phytopathology*; I.K. International Publishing House Pvt Ltd.: New Delhi, India, 2016.

84. Bishop, A.C.; Sun, T.; Johnson, M.E.; Bruno, V.M.; Patton-Vogt, J. Robust utilization of phospholipase-generated metabolites, glycerophosphodiesters, by *Candida albicans*: Role of the CaGit1 permease. *Eukaryot. Cell* **2011**, *10*, 1618–1627. [CrossRef]

85. Bishop, A.C.; Ganguly, S.; Solis, N.V.; Cooley, B.M.; Jensen-Seaman, M.I.; Filler, S.G.; Mitchell, A.P.; Patton-Vogt, J. Glycerophosphocholine utilization by *Candida albicans*: Role of the Git3 transporter in virulence. *J. Biol. Chem.* **2013**, *288*, 33939–33952. [CrossRef] [PubMed]

86. Sánchez-Vallet, A.; Tian, H.; Rodriguez-Moreno, L.; Valkenburg, D.J.; Saleem-Batcha, R.; Wawra, S.; Kombrink, A.; Verhage, L.; de Jonge, R.; van Esse, H.P.; et al. A secreted LysM effector protects fungal hyphae through chitin-dependent homodimer polymerization. *PLoS Pathog.* **2020**, *16*, e1008652. [CrossRef]

87. Pazzagli, L.; Cappugi, G.; Manao, G.; Camici, G.; Santini, A.; Scala, A. Purification, characterization, and amino acid sequence of cerato-platanin, a new phytotoxic protein from *Ceratocystis fimbriata* f. sp. platani. *J. Biol. Chem.* **1999**, *274*, 24959–24964. [CrossRef]

88. Sbrana, F.; Bongini, L.; Cappugi, G.; Fanelli, D.; Guarino, A.; Pazzagli, L.; Scala, A.; Vassalli, M.; Zoppi, C.; Tiribilli, B. Atomic force microscopy images suggest aggregation mechanism in cerato-platanin. *Eur. Biophys. J.* **2007**, *36*, 727–732. [CrossRef]

89. Cai, F.; Gao, R.; Zhao, Z.; Ding, M.; Jiang, S.; Yagtu, C.; Zhu, H.; Zhang, J.; Ebner, T.; Mayrhofer-Reinhartshuber, M.; et al. Evolutionary compromises in fungal fitness: Hydrophobins can hinder the adverse dispersal of conidiospores and challenge their survival. *ISME J.* **2000**, *14*, 2610–2624. [CrossRef]

90. Sakamoto, Y.; Watanabe, H.; Nagai, M.; Nakade, K.; Takahashi, M.; Sato, T. *Lentinula edodes tlg1* encodes a thaumatin-like protein that is involved in lentinan degradation and fruiting body senescence. *Plant Physiol.* **2006**, *141*, 793–801. [CrossRef]

91. Grenier, J.; Potvin, C.; Trudel, J.; Asselin, A. Some thaumatin-like proteins hydrolyse polymeric beta-1,3-glucans. *Plant J.* **1999**, *19*, 473–480. [CrossRef]
92. Fujimoto, H.; Aoyama, H.; Noguchi-Yachide, T.; Hashimoto, Y.; Kobayashi, H. Fusarielin A as an anti-angiogenic and anti-proliferative agent: Basic biological characterization. *Chem. Pharm. Bull.* **2008**, *56*, 298–304. [CrossRef] [PubMed]